DOI: 10.1007/s10856-014-5280-7

J Mater Sci: Mater Med (2014) 25:2357–2363
DOI 10.1007/s10856-014-5280-7

Apatite bone cement reinforced with calcium silicate fibers

Mariana Motisuke · Verônica R. Santos · Naiana C. Bazanini · Celso A. Bertran

Received: 13 December 2013 / Accepted: 16 July 2014 / Published online: 23 July 2014

Abstract Several research efforts have been made in the attempt to reinforce calcium phosphate cements (CPCs) with polymeric and carbon fibers. Due to their low compatibility with the cement matrix, results were not satisfactory. In this context, calcium silicate fibers ($CaSiO_3$) may be an alternative material to overcome the main drawback of reinforced CPCs since, despite of their good mechanical properties, they may interact chemically with the CPC matrix. In this work $CaSiO_3$ fibers, with aspect ratio of 9.6, were synthesized by a reactive molten salt synthesis and used as reinforcement in apatite cement. 5 wt.% of reinforcement addition has increased the compressive strength of the CPC by 250 % (from 14.5 to 50.4 MPa) without preventing the cement to set. Ca and Si release in samples containing fibers could be explained by $CaSiO_3$ partial hydrolysis which leads to a quick increase in Ca concentration and in silica gel precipitation. The latter may be responsible for apatite precipitation in needle like form during cement setting reaction. The material developed presents potential properties to be employed in bone repair treatment.

M. Motisuke (✉) · V. R. Santos · N. C. Bazanini
Bioceramics Laboratory - Science and Technology Institute, UNIFESP, 330 Talim Street - Vila Nair, São José dos Campos, SP, Brazil
e-mail: motisuke@unifesp.br

C. A. Bertran
Physical Chemistry Department, Institute of Chemistry, UNICAMP, Campinas, SP, Brazil

1 Introduction

Calcium phosphate cements (CPCs) have high biocompatibility with the human body due to its similarity to the mineral part of bone. Therefore, they are excellent materials for repairing bone defects [1–9]. CPCs are composed of a calcium phosphate powder and a liquid which mixture leads to a moldable paste that has low-temperature setting reaction [4, 5]. Once in contact with the liquid, the powder component dissolves and a new compound precipitates; apatite ($Ca_{10}(PO_4)_6(OH)_2$) or brushite ($CaHPO_4.H_2O$) depending on the pH [6, 9]. Material hardens spontaneously in minutes due to crystal entanglement.

Despite their excellent biological properties, CPCs are extremely brittle which restricts their use in small defects on no load bearing locations [4, 6, 9]. Potential applications of CPCs can be broaden by the addition of structural reinforcements to the compound matrix as polymeric and carbon fibers [6, 9–12]. Nevertheless, due to their low compatibility with the cement matrix, the results were not satisfactory. Buchanan et al. [12] added 1.5–10 wt.% of polypropylene fibers to an α-TCP cement and obtained compressive strengths ranging from 7 to 10.5 MPa, values close to the lower limit of the trabecular bone (1.5–45 MPa) [6].

Krüger and Groll [9] summarized the key factors for fiber reinforced CPCs. Besides fiber aspect ratio, orientation, interface and fiber roughness; biocompatibility, bioactivity and degradation rate are properties that are underlining the development of new reinforced cements. In fact, in order to promote bone tissue growth through the implant it is crucial to employ degradable and bioactive fibers. Bioceramic fibers and whiskers may completely fill the key factors underlined by Kruger and Groll since they have good interface compatibility with CPCs, could be

synthesized with large aspect ratio (length to diameter ratio, L/D) and have high strength modulus.

Müller et al. [13] employed hydroxypatite whiskers to reinforce an apatite bone cement. It was observed that with an addition of 30 % in volume of whiskers, the fracture toughness increased about 57 %. However, with higher quantities of reinforcement the material became more fragile. In the same work, the influence of reinforcement morphology was investigated. The authors added to the bone cement matrix spherical hydroxyapatite particles in sufficient quantity to achieve the same specific area when 30 % in volume of whiskers were added. It was verified that the increase on fracture toughness was only of 15 %. Thus, the enhancement of mechanical properties in composite materials is related, mainly, to the geometrical morphology and quantity of reinforcement [13].

Although bioceramic fibers and whiskers may have paramount mechanical strength and interface compatibility with CPCs, its synthesis is challenging. The methodologies commonly employed like hydrothermal method [14], decomposition of chelating agents [15] and microemulsions [16] are not feasible in large scale due to their complexity and high costs of precursors. Moreover, this processes usually lead to materials with low crystallinity, low aspect ratio and, mainly, low purity leading to composites with low biocompatibility and bioactivity [17].

On the other hand, molten salt synthesis (MSS) [18, 19], which has been employed on the preparation of ceramic fibers and whiskers used as catalyst supports, presents simpler processes, lower costs, large scale production and properties control. This method is a simple way to synthesize ceramic fibers and whiskers by employing a mixture of alkaline salts and the ceramic precursors, which are heated until the formation of a flux. This flux gives the ceramic particles the mobility and solubility needed to promote whisker/fiber growth [20]. The morphology and aspect ratio of the material is dependent of synthesis temperature, alkaline flux composition and size distribution of the ceramic precursors [18, 20–23]. Compared to conventional ceramic solid state reaction, MSS is a better option since it employs lower temperatures and guarantees particle size control [19, 24].

Therefore, calcium silicate in fibrous form have the required properties to be added into CPCs, since it shows high biocompatibility, bioactivity, resorbability and strength modulus [6, 25, 26]. Hayashi et al. [18] synthesized *wollastonite* whiskers by MSS using nanosized calcium silicate, NaCl and KCl. They obtained aspect ratios ranging from 7.1 to 21.7; and decreasing sizes of whiskers with the increasing of the heating temperature. Moreover, authors inferred that whisker growth only take place when starting materials were very fine.

Our group has published a similar method for producing calcium silicate fibers [22]. We employed a reactive MSS where $CaCO_3$ and fumed SiO_2 were intimately mixed with a NaCl/KCl flux and heated at 950 °C for different periods of time. The results showed that the longer the dwell time and the heating rate were, the more efficient the process was (i.e. greater the aspect ratio and reaction yield). Further studies were carried out and we were able to obtain $CaSiO_3$ fibers with aspect ratio close to 10, with very homogeneous morphology and crystalline phase purity [27].

Based on the statements above, this work aims to develop an apatite bone cement reinforced by calcium silicate ($CaSiO_3$) fibers which may enhance the chemical interaction between reinforcement and CPC matrix.

2 Materials and methods

2.1 Calcium silicate fibers

Calcium silicate ($CaSiO_3$) fibers were synthesized by a reactive molten salt method [22, 27] employing calcium carbonate ($CaCO_3$, Sigma-Aldrich) and electronic grade silicon dioxide (fumed SiO_2, Sigma-Aldrich) as precursors. Reactants were intimately milled and mixed with a mortar and pestle at stoichiometric proportion to form $CaSiO_3$, as described by Eq. (1).

$$CaCO_3 + SiO_2 \rightarrow CaSiO_3 + CO_2 \quad (1)$$

Alkaline flux was prepared by mixing, at 1:1 weight ratio, NaCl (Synth, Brazil) and KCl (Synth, Brazil). Afterwards, calcium silicate precursors were homogenized with the alkaline flux at 1:6 weight ratio and then heated at 950 °C with a heating rate of 2 °C min^{-1} and dwell time of 12 h. After the heating treatment, samples were cooled inertially inside the furnace and washed with deionized water at 80 °C under vigorously stirring for 1 h. The supernatant was changed and the process was repeated until its conductivity was equal to the deionized water. Finally, fibers were filtered and dried at 100 °C overnight.

2.2 CPC samples

CPC solid phase, α-TCP, was synthesized by solid state reaction at 1,300 °C of a 2:1 molar ratio mixture of "Mg-free" $CaHPO_4$ and $CaCO_3$ [8, 28] followed by ball milling during 96 h (zirconia milling media of 10 and 15 mm of diameter and ball/powder weight ratio of 10:1). The resulting powder was analyzed by laser diffraction (CILAS 1190) and surface area analyzer (Quantachrome, NOVA 4200e) and presented a mean particle size of 4.93 μm, a particle size distribution between 1.33 and 10 μm and a

Table 1 CPC samples nomenclature, composition and setting times

Nomenclature	Fibers (wt.%)	L/P (mL g^{-1})
A0W	0	0.40
A5W	5	0.42
A10W	10	0.44

surface area of 4.7 m^2 g^{-1}. The liquid phase of the CPC was a 2.5 % Na_2HPO_4 (Synth, Brazil) aqueous solution.

Cement samples were prepared by adding 0, 5 and 10 wt.% of $CaSiO_3$ fibers to the α-TCP powder. Liquid-to-powder ratio (L/P) was determined to each sample in order to maintain cement paste moldability. Table 1 describes cement samples nomenclature, fibers wt.% and L/P employed.

Cement pastes were prepared by mixing by hand the liquid and the powder during 1 min; then pastes were molded into Teflon® molds of 6 × 12 mm. After 30 min of being molded, samples were immersed in Ringer's solution during 7 days at 36.5 °C to complete the setting reaction. Afterwards, samples were washed with distilled water and dried in air overnight. Finally, the surface of the samples was smoothen with an emery paper to make it flat and then they were demolded.

2.3 Characterization

2.3.1 X-ray diffraction (XRD)

Crystalline phase analyses of α-TCP, calcium silicate fibers and cement samples were carried out by means of X-ray diffraction (XRD) (X'Pert Pro, PANalytical, X'Celerator, CuKα, Ni filter, 10°–40° (2θ), 0.02° s^{-1}, 45 kV, 40 mA).

2.3.2 BET surface area

Fibers surface area was determined in a surface area analyser (Quantachrome, NOVA 4200e).

2.3.3 Compressive strength

At least six specimens of each cement formulation (A0, A5 and A10 W) were mechanically tested in a universal testing machine (EMIC DL20000, tesc version 3.04, 10kN cell) with a crosshead speed of 0.5 mm min^{-1}.

2.3.4 Scanning electron microscopy (SEM)

Fibers were dispersed in isopropyl alcohol, sonicated for 30 min and a tiny drop was left to dry on the sample-holder surface. Fibers' morphology and aspect ratio and the surface of fracture of the cements samples were analyzed by scanning electron microscopy (FEI Inspect 5S). Samples were coated with Au–Pd (Bal-Tec MCS010).

2.3.5 Ionic release

Calcium, phosphorus and silicon release of fibers and cements were evaluated in triplicate during different periods of time (3, 6, 12, 24, 48 and 168 h). Samples were immersed in a 0.05 mol L^{-1} HNO_3/tris buffer solution (pH = 7.4) at 36.5 °C with a sample weight (g) and buffer volume (mL) ratio of 1:100. Cement pastes were prepared with the same composition described in item 2.2 and buffer was added only after 30 min of mixing to ensure cement's cohesion.

After each period of time, 3.00 mL of the solution in contact with the samples was collected in a syringe and filtered with a 0.45 μm filter to remove all the solid material that could influence on the determination of ionic concentration. Afterwards, the resulting liquid was diluted in a 0.05 mol L^{-1} HNO_3 solution and ionic concentration was measured by ICP-OES (Pelkin Elkmer, Optima 3000DV).

2.3.6 Statistics

One-way analysis of variances (ANOVA) has been performed on Minitab® release 14.1 to compare differences between the mean values of samples' compressive strength using a confidence level of 95 %. Tukey's comparison post hoc test was performed to assess differences in each pair of means.

Normality and equal variances tests were conducted prior to ANOVA to guarantee that data followed Normal distribution and presented homoscedasticity.

3 Results

The method proposed was efficient in obtaining calcium silicate fibers with aspect ratio (L/D) of 9.6 as seen in SEM micrograph of Fig. 1. The crystalline phase of calcium silicate formed during the synthesis was *parawollastonite* (JCPDS 43-1460) as displayed on XRD pattern of Fig. 2. No evidence of precursors or alkaline flux was identified. Fibers BET surface area was 4.7 m^2 g^{-1}.

Fibers did not prevent cement setting reaction as in all formulations α-TCP was converted into apatite after 7 days of setting, as seen on XRD patterns of Fig. 2. Nevertheless, apatite morphology was influenced by the presence of the fibers since for samples A5W and A10W apatite has precipitated in needle like form while in sample A0W apatite crystals were in plate like form (Fig. 3). Moreover, for samples containing fibers it is possible to verify the

presence of the fibers that is indicated by the white arrows in SEM micrographs of Fig. 3.

Compressive strength (Fig. 4) has increased by 250 % (from 14.5 to 50.4 MPa) when fiber addition was 5 wt.%. By increasing reinforcement to 10 wt.% mechanical resistance started to decrease, but still higher when compared to the sample with no fiber addition (32.3 MPa). ANOVA results revealed a p value < 0.05. Tukey's comparison test yield to significant difference between the compressive strength of samples.

Samples' Ca, P and Si release as a function of time is reported in Fig. 5. For calcium silicate fibers Ca and Si concentration after 168 h reached 675 and 18 mg L^{-1}, respectively. P concentration for all cement samples presented a similar behavior, reaching a maximum value around 24 h and then decreasing during the rest of the assay. Nevertheless, fibers has influenced on cements' Ca release since as higher the calcium silicate content smaller is the decrease in Ca concentration after 24 h. For instance, for sample A10W Ca concentration increased continuously without reaching a maximum during the period analyzed.

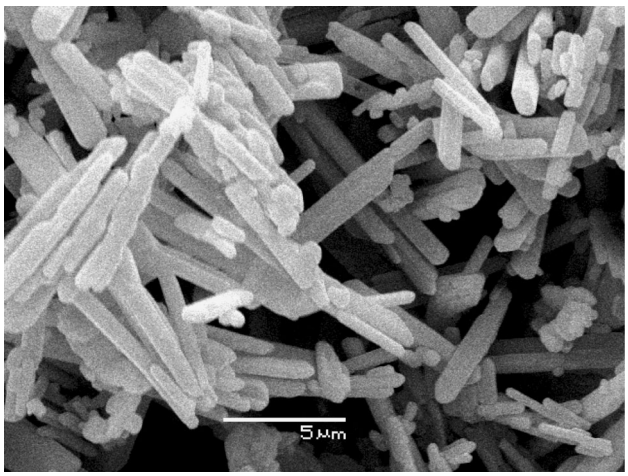

Fig. 1 SEM micrographs of $CaSiO_3$ fibers. Reactive molten salt synthesis led to fibers with aspect ratio of 9.6

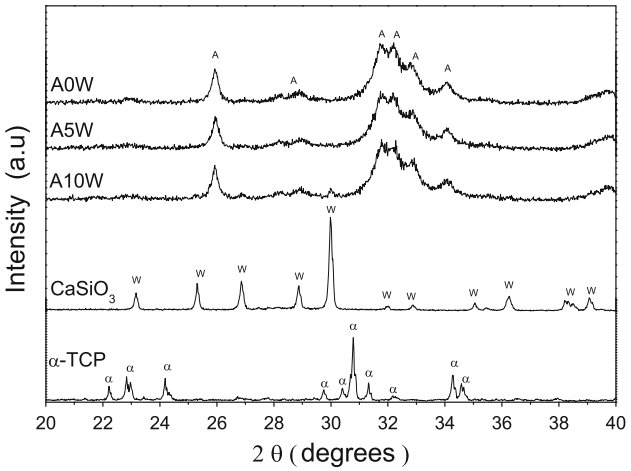

Fig. 2 XRD patterns of as-prepared $CaSiO_3$ fibers, α-TCP and cements samples. *Legend* W—$CaSiO_3$, α—α-TCP and A—apatite

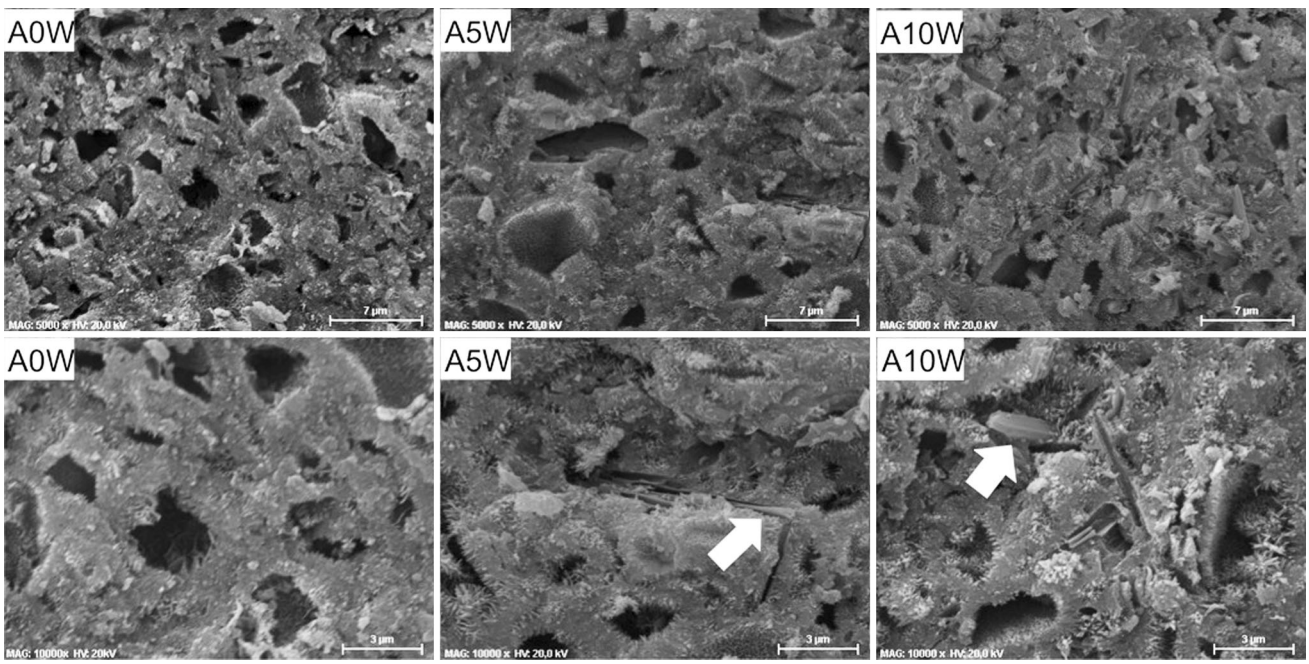

Fig. 3 SEM micrographs of surface of fracture of cement samples. *White arrows* indicate the presence of the fibers

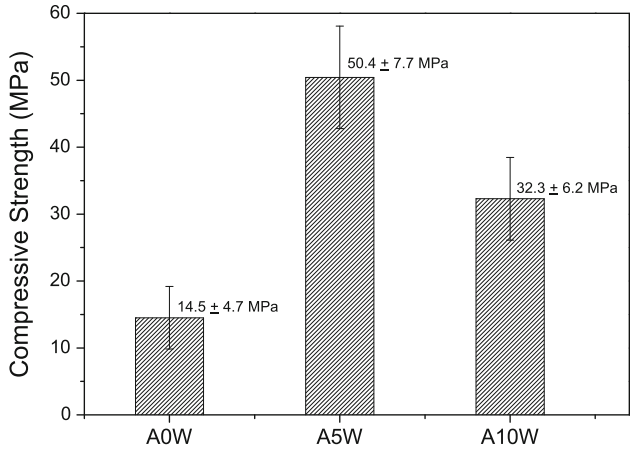

Fig. 4 Compressive strength of samples. Fibers addition increased samples' compressive strength (ANOVA, $p < 0.05$)

4 Discussion

Needle-like and crystalline calcium silicate fibers were obtained by a simple reactive MSS. The growth of the fibers was preferred in [−3 2 0] direction since in Fig. 2 the relative intensities of the XRD lines present a small deviation when compared to JCPDS pattern (43−1460), i.e. other diffraction lines, besides [−3 2 0], present lower relative intensity in the XRD pattern of the as synthesized fibers when compared to JCPDS pattern. Moreover, MSS allowed calcium silicate formation at lower temperatures. We achieved 100 % of reaction yield at 950 °C while other researchers report that calcium silicate with high crystalline phase purity is only obtained after heat treatment at 1,400 °C [29].

The method proposed in this work presents advantages when compared to the one once published by Hayashi et al. [18].

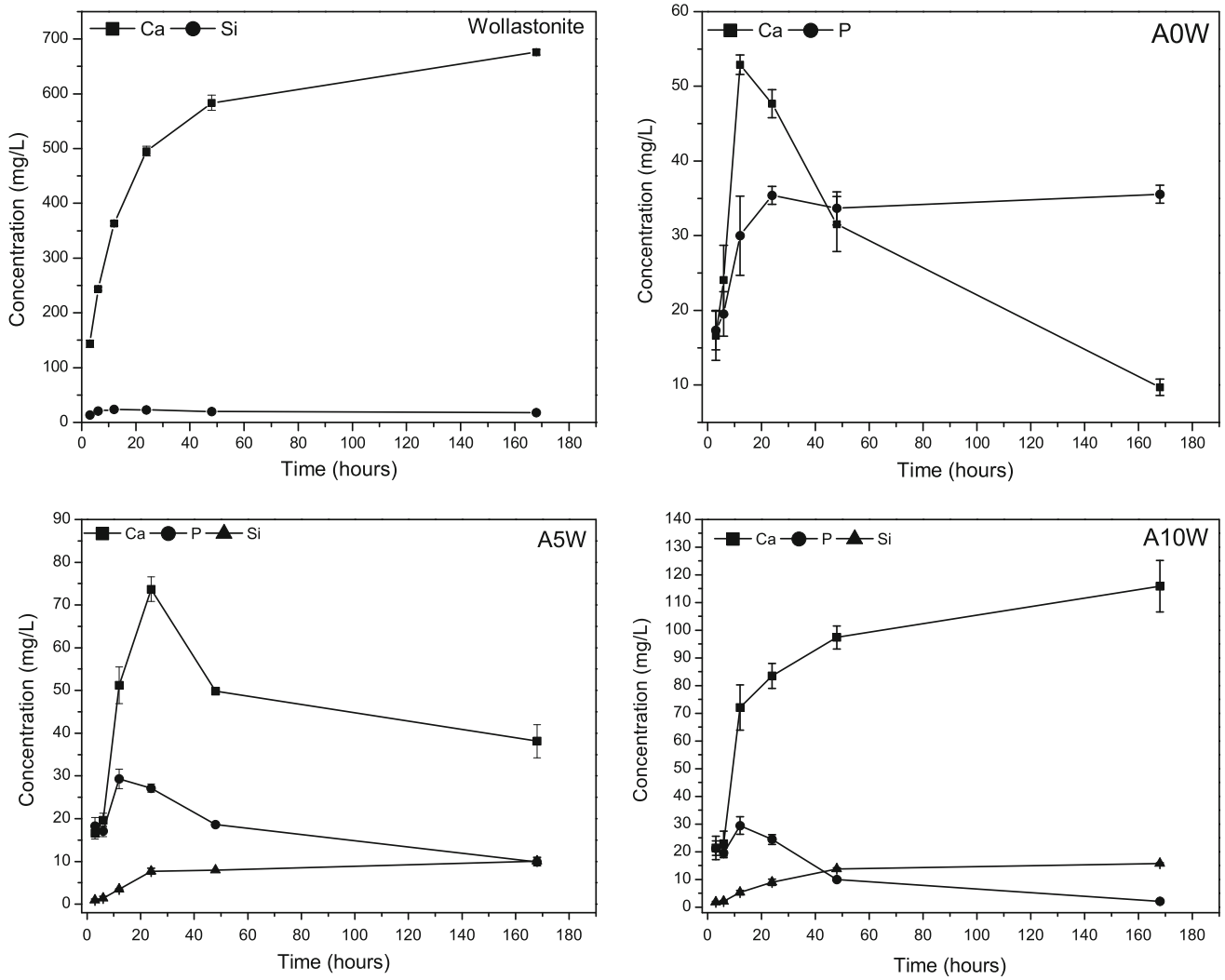

Fig. 5 Ca, P and Si release of wollastonite fibers, A0W, A5W and A10W

We obtained a similar average aspect ratio using a lower powder to alkaline flux ratio (1:6 against 1:40) and a lower dwell time (12 h against 24 h). Moreover it was not necessary to control cooling rate.

Cement setting reaction took place as expected once all α-TCP was converted into apatite even with 10 wt.% of fiber reinforcement as can be observed in all XRD patterns from Fig. 2. For sample A10W calcium silicate was identified in XRD pattern (Fig. 2) confirming that reinforcement did not take part on cement setting reaction and did not lead to the formation of any other crystalline phase.

As observed in Fig. 4, increment of compressive strength presents a maximum value (increase of 250 %) when 5 wt.% of fibers was added into CPC matrix and decreases when 10 wt.% is added (increase of 123 %). These values reaches the upper limit of trabecular bone (45 MPa) [6]. Some works report the reinforcement of α-TCP cement by adding polypropylene [12] and Nylon 66 [30] fibers and compressive strengths ranging from 7 to 10.5 MPa and 8.5 to 12.5 MPa were obtained, respectively. Those values are very close to the lower limit of trabecular bone (1.5 MPa) [6].

In this work, besides reinforcing the CPC matrix by presenting great strength modulus, $CaSiO_3$ fibers seem to have influenced on the morphology of apatite crystals that have precipitated during cement setting reaction. Indeed, in SEM micrographs of Fig. 3, apatite crystals are smaller and present a more homogeneous needle-like morphology in samples in which reinforcement was added. This promotes a more efficient crystal entanglement leading to an increase in mechanical resistance.

Furthermore, the partial calcium silicate fibers hydrolysis (Eq. 2) was responsible for Ca and Si concentration increase during ionic release experiment. As observed in Fig. 5, for all periods of time, fibers and reinforced samples presented higher values of calcium concentration when compared to no reinforced cement.

$$CaSiO_3 + 2H^+ + H_2O \rightleftharpoons Ca^{2+} + H_4SiO_4 \quad (2)$$

As reported by Rimstidt and Dove [31], calcium silicate hydrolysis is fast, leading to a quick increase in Ca and Si concentration. Nevertheless, as part of the silicic acid (H_4SiO_4) formed reacts to form silica gel (SiO_2, Eq. (3)), Si content after 168 h is not as high as Ca concentration.

$$H_4SiO_4 \rightleftharpoons SiO_2 + 2H_2O \quad (3)$$

Silica gel (or silica-rich layer) induces apatite precipitation on the surface of bioglasses and related biomaterials by incorporating Ca and P from the interface environment [32–34]. The well accepted mechanism for biomineralization, proposed by Hench [35], demonstrates the ability of silica gel to stimulates the nucleation and growth of small apatite crystals with needle like morphology. The same morphology was observed in samples A5W and A10W after cement was kept in Ringer's solution to set. Therefore, fibers have probably induced apatite precipitation in needle like form due to calcium silicate hydrolysis [31, 33].

5 Conclusion

It was possible to reinforce an apatite cement by adding 5 wt.% of calcium silicate fibers. Fibers were obtained by a reactive MSS with an aspect ratio of 9.6. Compressive strength has increased by 250 % and reinforcement presence did not prevent cement setting reaction. Ca and Si release in samples A5W and A10W could be explained by $CaSiO_3$ hydrolysis that leads to a quick increase in Ca concentration and in silica gel precipitation. The latter may be responsible for apatite precipitation in needle like form during cement setting reaction. The material developed present potential properties to be employed in bone repair treatment.

Acknowledgments The authors would like to thank The São Paulo Research Foundation (FAPESP) for the financial support (Processes numbers 2011/09240-9 and 2012/07556-1) and Dr. João Paulo Barros Machado from the Laboratory of Sensors and Materials (LAS) of the National Institute of Space Research (INPE) for kindly providing the XRD analysis.

References

1. Brown WE, Chow LC. A new calcium phosphate setting cement. J Dent Res. 1983;62(1 suppl):606-693.
2. LeGeros RZ. Calcium phosphates in oral biology and medicine. 1st ed. New York: Karger; 1991. p. 201.
3. Bohner M. Calcium orthophosphates in medicine: from ceramics to calcium phosphate cements. Injury. 2000;31(4):D37–47.
4. Dorozhkin SV. Calcium orthophosphate cements and concretes. Materials (Basel). 2009;2:221–91.
5. Ginebra MP, Espanol M, Montufar EB, Perez RA, Mestres G. New processing approaches in calcium phosphate cements and their applications in regenerative medicine. Acta Biomater. 2010;6:2863–73.
6. Canal C, Ginebra MP. Fibre-reinforced calcium phosphate cements: a review. J Mech Behav Biomed Mater. 2011;4:1658–71.
7. Motisuke M, Carrodeguas RG, de Zavaglia CAC. Si-tricalcium phosphate cement: preparation, characterization and bioactivity in SBF. Mater Res. 2011;14:493–8.
8. Motisuke M, Carrodeguas RG, de Zavaglia CAC. Si-TCP synthesized from "Mg-free" reagents employed as calcium phosphate cement. Mater Res. 2012;15:568–72.
9. Krüger R, Groll J. Fiber reinforced calcium phosphate cements—on the way to degradable load bearing bone substitutes? Biomaterials. 2012;33:5887–900.
10. De Oliveira LC, Cristina E, dos Santos LA, Rigo ECS, Carrodeguas RG, Boschi AO, et al. Fiber reinforced calcium phosphate cement. Artif Organs. 2000;24:212–6.
11. Dos Santos LA, Carrodeguas RG, Boschi AO, de Arruda AC. Dual-setting calcium phosphate cement modified with ammonium polyacrylate. Artif Organs. 2003;27:412–8.

12. Buchanan F, Gallagher L, Jack V, Dunne N. Short-fibre reinforcement of calcium phosphate bone cement. Proc Inst Mech Eng Part H. 2007;221:203–11.
13. Müller FA, Gbureck U, Kasuga T, Mizuysni Y, Barralet JE, Lohbauer U, et al. Whisker-reinforced calcium phosphate cements. J Am Ceram Soc. 2007;90:3694–7.
14. Kobayashi M, Petrykin V, Kakihana M, Tomita K. Hydrothermal synthesis and photocatalytic activity of whisker-like rutile-type titanium dioxide. J Am Ceram Soc. 2009;92:S21–6.
15. Kandori K, Horigami N, Yasukawa A, Ishikawa T. Texture and formation mechanism of fibrous calcium hydroxyapatite particles prepared by decomposition of calcium-EDTA chelates. J Am Ceram Soc. 2005;80:1157–64.
16. Lin K, Chang J, Lu J. Synthesis of wollastonite nanowires via hydrothermal microemulsion methods. Mater Lett. 2006;60: 3007–10.
17. Yoshimura M, Suda H, Okamoto K, Ioku K. Hydrothermal synthesis of biocompatible whiskers. J Mater Sci. 1994;29: 3399–402.
18. Hayashi S, Sugai M, Nakagawa Z, Takei T, Kawasaki K, Katsuyama T, et al. Preparation of $CaSiO_3$ whiskers from alkali halide fluxes. J Eur Ceram Soc. 2000;20:1099–103.
19. Yoon KH, Cho YS, Kang DH. Review Molten salt synthesis of lead-based relaxors. J Mater Sci. 1998;33:2977–84.
20. Afanasiev P, Geantet C. Synthesis of solid materials in molten nitrates. Coord Chem Rev. 1998;178–180:1725–52.
21. Jalota S, Bhaduri SB, Tas AC. In vitro testing of calcium phosphate (HA, TCP, and biphasic HA-TCP) whiskers. J Biomed Mater Res A. 2006;78:481–90.
22. Motisuke M, Bertran CA. Síntese de "whiskers" de $CaSiO_3$ em fluxo salino para elaboração de biomateriais. Cerâmica. 2012;58: 504–8.
23. Ramos SLF, Motisuke M, Rodrigues LR, Zavaglia CAC. Whisker-like hydroxyapatite synthesized by molten salt synthesis (MSS) of nano-hydroxyapatite in a KCl/NaCl Flux. Key Eng Mater. 2009;396–398:497–500.
24. Taş AC. Molten salt synthesis of calcium hydroxyapatite whiskers. J Am Ceram Soc. 2004;84:295–300.
25. Bose S, Tarafder S, Banerjee SS, Davies NM, Bandyopadhyay A. Understanding in vivo response and mechanical property variation in MgO, SrO and SiO_2 doped β-TCP. Bone. 2011;48:1282–90.
26. De Aza PN, Guiten F, de Aza S. Bioactivity of wollastonite bioceramics: in vitro evaluation. Scr Met Mat 1994;31:1001-1005.
27. Dos Santos VR, Bertran CA, Motisuke M. Obtenção de "whiskers" de wollastonita para reforço de biomateriais. Natal: An. do VII Congr. Lat. Am. Orgãos Artif. e Biomateriais; 2012.
28. Motisuke M, Carrodeguas RG, Zavaglia CAC. Mg-free precursors for the synthesis of pure phase Si-doped α-$Ca_3(PO_4)_2$. Key Eng Mater. 2008;361–363:199–202.
29. De Aza PN, Guitián F, De Aza S, Valle FJ. Analytical control of wollastonite for biomedical applications by use of atomic absorption spectrometry and inductively coupled plasma atomic emission spectrometry. Analyst. 1998;123:681–5.
30. Dos Santos LA, Carrodeguas RG, Boschi AO, Carrodéguas RG. Fonseca de Arruda AC. Fiber-enriched double-setting calcium phosphate bone cement. J Biomed Mater Res, Part A. 2003;65: 244–50.
31. Rimstidt JD, Dove PM. Mineral/solution reaction rates in a mixed flow reactor: wollastonite hydrolysis. Geochim Cosmochim Acta. 1986;50:2509–16.
32. Pereira MM, Hench LL. Mechanisms of hydroxyapatite formation on porous gel–silica substrates. J Sol–Gel Sci Technol. 1996;7:59–68.
33. Liu X, Ding C, Chu PK. Mechanism of apatite formation on wollastonite coatings in simulated body fluids. Biomaterials. 2004;25:1755–61.
34. Pereira MM, Clark AE, Hench LL. Calcium phosphate formation on sol–gel-derived bioactive glasses in vitro. J Biomed Mater Res. 1994;28:693–8.
35. Hench LL. Bioceramics: from concept to clinic. J Am Ceram Soc. 1991;74:1487–510.